Organic LETTERS

Letter

pubs.acs.org/OrgLett

Euphomilones A and B, ent-Rosane Diterpenoids with 7/5/6 and 5/7/6 Skeletons from *Euphorbia milii*

Shao-Nan Liu,[†,⊥] Dane Huang,[†,⊥] Susan L. Morris-Natschke,[‡] Hang Ma,[§] Zhi-hong Liu,[†] Navindra P. Seeram,[§] Jun Xu,[†] Kuo-Hsiung Lee,[‡,∥] and Qiong Gu*[,†]

[†]Research Center for Drug Discovery, School of Pharmaceutical Sciences, Sun Yat-sen University, Guangzhou 510006, People's Republic of China

[‡]Natural Products Research Laboratories, UNC Eshelman School of Pharmacy, University of North Carolina, Chapel Hill, North Carolina 27599, United States

[§]Bioactive Botanical Research Laboratory, Department of Biomedical and Pharmaceutical Sciences, College of Pharmacy, University of Rhode Island, Kingston, Rhode Island 02881, United States

[∥]Chinese Medicine Research and Development Center, China Medical University and Hospital, Taichung, Taiwan

Supporting Information

ABSTRACT: Three highly modified *ent*-rosane diterpenoids, euphomilones A (**1**) and B (**2**) and euphomianol A (**3**), were isolated from the aerial parts of *Euphorbia milii*. The structures were elucidated from physical, spectroscopic, and X-ray diffraction data, as well as experimental and calculated electronic circular dichroism (ECD) analysis. Plausible biogenetic pathways to **1**−**3** are proposed. Also, compound **1** exhibited inhibition of receptor activator of nuclear factor-kappaB ligand (RANKL)-induced osteoclast formation (IC_{50} = 12.6 μM).

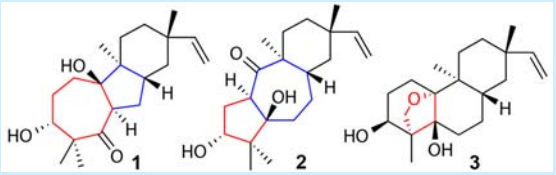

Euphorbia, the largest genus of the Euphorbiaceae family, is characterized by the production of a milky irritant latex[1] and is well-known for producing secondary metabolites with immense chemical diversity.[2,3] Euphorbia species have been used for the treatment of skin diseases, gonorrhea, migraine, intestinal parasites, and warts.[4] Various types of natural products, including sesquiterpenoids, diterpenoids, triterpenoids, flavonoids, and steroids, have been isolated from this genus. However, diterpenoids with different cyclic systems, including ingenane, jatrophane, tigliane, abietane, and atisane, predominate.[2] Euphorbia diterpenoids are reported to exhibit many biological activities, including antitumor, multidrug-resistance-reversing, anti-inflammatory, and anti-HIV properties.[5] Notably, ingenol 3-angelate (ingenol mebutate, PEP005, Picato, LEO Pharma), an ingenane diterpene isolated from *Euphorbia peplus*, was approved by the US FDA in 2012 for the treatment of actinic keratosis, a precancerous skin condition.[6]

Euphorbia milii is mainly distributed in the southwestern areas of China, such as Guangdong, Guangxi, Fujian, Yunnan, and Guizhou Provinces. The stem, root, and latex of this plant are used as a detoxicant in traditional Chinese herbal medicine.[7] As part of our continuing study on the structurally unique and bioactive constituents from medicinal plants,[8−11] we investigated *E. milii* and discovered three new *ent*-rosane diterpenoids featuring a novel 7/5/6 fused-ring system (euphomilone A, **1**), a 5/7/6 tricyclic system (euphomilone B, **2**), and a 10,19-oxygen bridge (euphomianol A, **3**) (Figure 1).

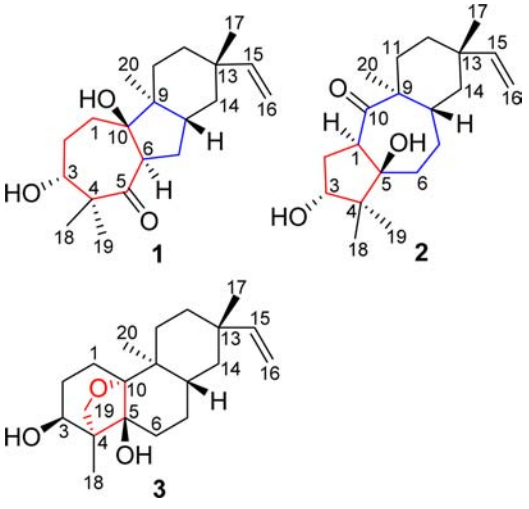

Figure 1. Structures of compounds **1**−**3**.

It is particularly noteworthy that, to the best of our knowledge, compound **1** is the first natural diterpenoid possessing a 7/5/6 tricyclic system. Compound **2** represents the first example of a rosane-type diterpenoid with a 5/7/6 fused ring system. The ether linkage between C-10 and C-19 of **3** is the first found in rosane-type diterpenoids. Moreover, **1** also exhibited significant inhibition against receptor activator of

Received: October 20, 2016
Published: November 22, 2016

DOI: 10.1021/acs.orglett.6b03142
Org. Lett. 2016, 18, 6132−6135

nuclear factor-kappaB ligand (RANKL)-induced osteoclast formation in RAW 264.7 cells.

Euphomilone A (**1**) was obtained as colorless crystals with a molecular formula of $C_{20}H_{32}O_3$ based on the HRESIMS ion at m/z 343.22406 $[M + Na]^+$ (calcd 343.22437), indicating five degrees of unsaturation. The IR absorptions at ν_{max} 3421 and 1685 cm^{-1} revealed the presence of hydroxyl and carbonyl groups. The ^1H NMR data (Table S1, Supporting Information) indicated the presence of four methyls (δ_H 1.01, 1.15, 1.15, and 0.78), a vinylic system (δ_H 5.83, dd, 10.7, 17.5 Hz; 4.85, d, 10.7 Hz; 4.93, d, 17.5 Hz), and two methines (δ_H 3.76, d, 6.9 Hz; 4.04, d, 10.4 Hz). The ^{13}C NMR data (Table S1, Supporting Information) and HMQC spectrum (Figure S6, Supporting Information) revealed 20 carbon resonances, including four methyls (δ_C 23.6, 25.7, 24.2, 14.5), a vinyl group (δ_C 151.0, 109.0), a ketone carbonyl group (δ_C 214.9), an oxygenated methine (δ_C 75.6), and an oxygenated tertiary carbon (δ_C 84.1). The aforementioned data suggested a possible pimarane- or rosane-type diterpenoid. These two skeletons differ in the position of CH_3-20. The CH_3-20 is positioned at C-9 in the rosane-type diterpenoid as opposed to its location at C-10 in the pimarane-type diterpenoid. This determination can be defined by the HMBC spectrum.[12] The HMBC spectrum of rosane-type diterpenoids exhibit correlations of H_3-20 with C-8 and C-11, which cannot be observed in that of pimarane-type diterpenoids. The HMBC correlation of H_3-20 (δ_C 0.78) with C-8 (δ_C 38.4), C-9 (δ_C 49.0), C-10 (δ_C 84.1), and C-11 (δ_C 26.4) indicated that CH_3-20 was located at C-9, which confirmed a rosane-type diterpenoid. HMBC correlations of H_3-19/18 (δ_H 1.15) with C-3 (δ_C 75.6), C-4 (δ_C 50.6), and the carbonyl carbon at δ_C 214.9 led to the assignment of the ketone carbonyl group at C-5. Based on the HMBC correlations of H-6 with C-1, C-5, C-8, and C-10, it was further apparent that the C_5-C_{10} bond was cleaved and a C_6-C_{10} bond was formed. Thus, the 2D structure of compound **1** was established as an unprecedented 7/5/6 tricyclic rosane-type diterpenoid.

The H_3-19/H_3-20/H-6 cross-peaks in the NOESY spectrum of **1** (Figure S8, Supporting Information) indicated their cofacial arrangement. Because no signals for 3-OH and 10-OH were present in the ^1H NMR spectrum in $CDCl_3$ (Figure S3, Supporting Information), the orientations of 3-OH and 10-OH could not be identified from the NOESY spectrum (Figure 2).

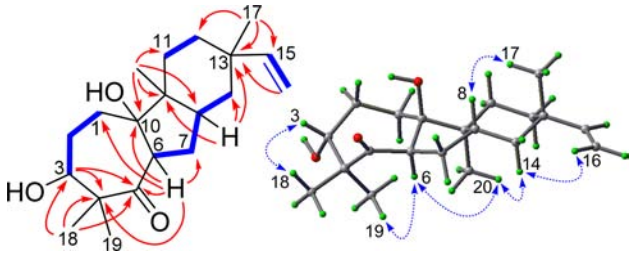

Figure 2. Key $^1H-^1H$ COSY (blue) and HMBC (red arrows) correlations and NOESY (double arrows) correlations of **1**.

Fortunately, crystals of compound **1** were obtained from *n*-hexane/EtOAc (2:1). Thus, the absolute stereochemistry of **1** was corroborated as 3*R*,6*R*,8*S*,9*S*,10*R*,13*S* (Figure 1) through a single crystal X-ray experiment with Cu Kα radiation [Figure 3; Flack parameter: −0.05 (14)].

Euphomilone B (**2**) was obtained as a colorless gum. Its molecular formula was determined as $C_{20}H_{32}O_3$ by HRESIMS at m/z 343.22398 $[M + Na]^+$ (calcd for $C_{20}H_{32}O_3Na$, 343.22437), requiring five degrees of unsaturation. The NMR data of **2** (Table S1, Supporting Information) were similar to those of **1**. Its ^{13}C NMR (Table S1, Supporting Information) disclosed four methyls, seven methylenes, four methines, three quaternary carbons, an oxygenated tertiary carbon, and a carbonyl group. Again, compound **2** possessed characteristic vinyl (δ_H 150.8, 109.3), ketone carbonyl (δ_C 213.9), oxygenated methine (δ_C 78.5), and oxygenated tertiary (δ_C 85.1) carbons. The aforementioned data indicated that compound **2** was also a rosane-type diterpenoid. The C-5 position was defined as an oxygenated tertiary carbon based on the observation of HMBC correlations between H_3-19 (δ_H 0.94) and carbons with chemical shifts at δ_C 78.5, 85.1, and 50.4. HMBC correlations from H-1 (δ_H 3.65, dd, 11.2, 4.7 Hz) to carbons with chemical shifts at δ_C 78.5, 85.1, 30.5, 213.9, and 33.4, as well as from H_3-20 (δ_H 1.05, s) to C-8 (δ_C 34.5), C-9 (δ_C 49.7), C-10 (δ_C 213.9), and C-11 (δ_C 29.6) revealed that C-10 was a ketone carbonyl group. The COSY correlations of H-1/H-2 and H-2/H-3 (Figure 4) indicated a $CH-CH_2-CH-O$ fragment. All of

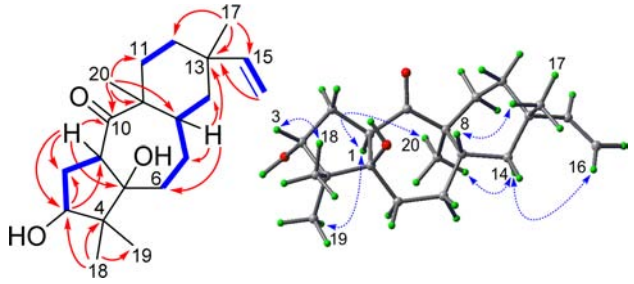

Figure 4. Key $^1H-^1H$ COSY (blue) and HMBC (red arrows) correlations and NOESY (double arrows) correlations of **2**.

the above data suggested the cleavage of the C_5-C_{10} bond and formation of the C_1-C_5 bond. Therefore, the planar structure of **2** was established as shown in Figure 1.

The relative configuration of **2** was determined via NOESY and NOE difference experiments. In the NOESY spectrum (Figure S16, Supporting Information), the H-1/H_3-19/H_3-20/H-14α/H-16 cross-peaks indicated that H-1/H_3-19/H_3-20 are cofacial, and they were assigned α-orientations. No hydroxy proton signals were observed in the ^1H NMR with $CDCl_3$ solvent (Figure S17, Supporting Information), and a ^1H NMR spectrum of **2** was taken in acetone-d_6 (Figure S11, Supporting Information). As shown in Figure S17 in Supporting Information, signals for two hydroxyls were observed at δ_H 3.66 (d, J = 5.6 Hz, 3-OH) and δ_H 2.95 (s, 5-OH). In the NOE

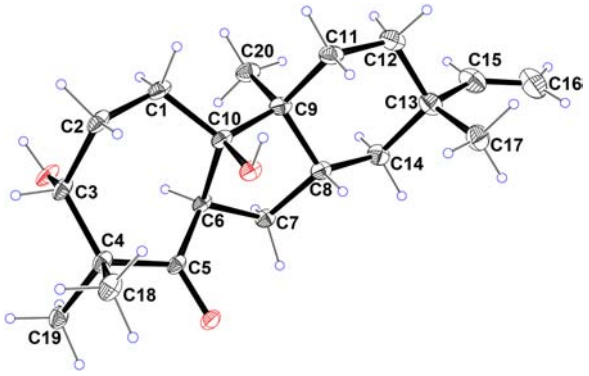

Figure 3. X-ray crystallographic structure of **1**.

DOI: 10.1021/acs.orglett.6b03142
Org. Lett. 2016, 18, 6132−6135

difference spectrum (Figure S17, Supporting Information), irradiation of H-3 caused enhancement of 3-OH and 5-OH, suggesting that H-3 and 5-OH are cofacial. In comparison to **1**, the relative configuration of **2** was defined as shown in Figure 1.

Biogenetically, 20-CH_3 and 17-CH_3 in **2** should likely have the same orientations as those in **1**. Thus, the absolute configuration of **2** was established as 1*R*,3*R*,5*R*,8*S*,9*S*,13*S*, which was supported by comparison of the experimental and calculated electronic circular dichroism (ECD) spectra (Figure 5).

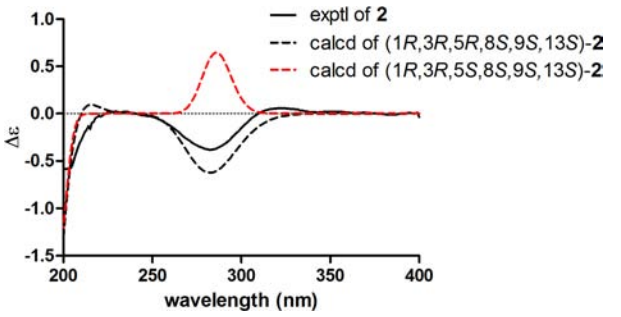

Figure 5. Calculated and experimental ECD spectra of **2**. The calculated ECD spectra were computed at the PBE1PBE/6-31++G(2d,2p) level in MeOH.

The molecular formula of **3** was deduced as $C_{20}H_{32}O_3$ based on the (+)-HRESIMS ion at *m*/*z* 343.22402 $[M + Na]^+$ (calcd 343.22437). The NMR data of **3** (Table S1, Supporting Information) showed the characteristic signals of rosane-type diterpenoids, except for the presence of a CH_2O group (δ_C 74.9) and the absence of one methyl group, which indicated that **3** was also a modified rosane-type diterpenoid. Detailed analysis of the HMBC and COSY correlations (Figure 6) revealed the 2D structure of **3** as shown in Figure 1.

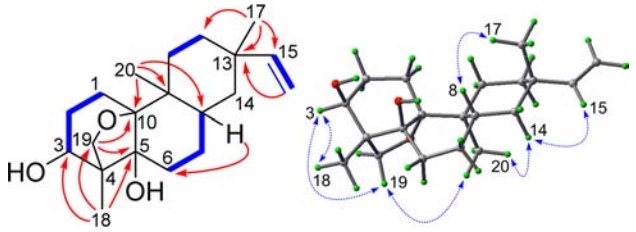

Figure 6. Key $^1H-^1H$ COSY (blue) and HMBC (red arrows) correlations and NOESY (double arrows) correlations of **3**.

The relative configuration of **3** was determined from a NOESY spectrum and comparison with the data of compounds **1** and **2**. In the NOESY spectrum (Figure S25, Supporting Information), the H-19/H_3-20 cross peaks indicated that H-19 has an α-orientation. From the configurations of C-9 and C-13 in **1** and **2**, 17-CH_3 and 20-CH_3 in **3** were assigned β- and α-orientations, respectively. A crystal of **3** was obtained from hexane/EtOAc (2:1) and subjected to an X-ray diffraction experiment with Cu Kα radiation [Figure 7; Flack parameter: −0.08 (12)]. Thus, the absolute configuration of **3** was assigned as 3*S*,4*R*,5*S*,8*S*,9*S*,10*R*,13*S* (Figure 1), and compound **3** was named euphomianol A.

Plausible biosynthetic pathways to **1**−**3** are postulated in Scheme 1. *ent*-Rosane, the primary rosane-type diterpene, is proposed as the biosynthetic precursor of the three

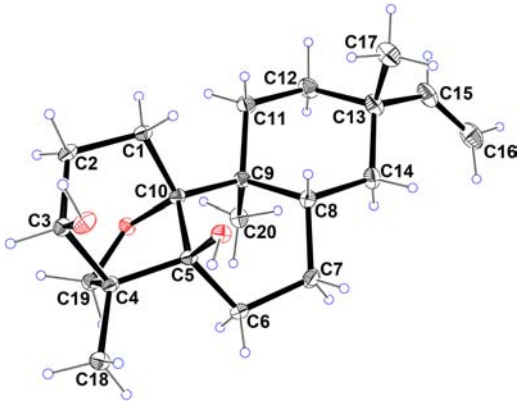

Figure 7. X-ray crystallographic structure of **3**.

Scheme 1. Plausible Biosynthetic Pathway of 1−3

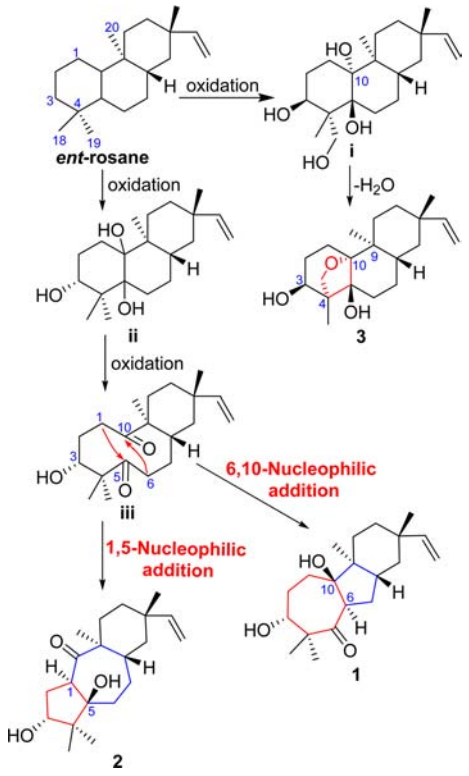

compounds. Oxidation of C-3, C-5, C-10, and C-19 of *ent*-rosane would yield the intermediate **i**, which could then lose H_2O to form the cyclic ether of compound **3**. Meanwhile, oxidation of C-3, C-5, and C-10 of *ent*-rosane would yield intermediate **ii**, which could be further transformed to **iii** via oxidative cleavage. Intermediate **iii** could be further converted into compounds **1** and **2** under basic conditions through 6,10-nucleophilic and 1,5-nucleophilic addition, respectively.

Compounds **1**−**3** were assayed for inhibition of RANKL-induced osteoclastogenesis in RAW 264.7 cell lines. Only compound **1** exhibited an inhibitory effect with an IC_{50} of 12.6 μM.

In summary, three new rosane-type diterpenoids with uncommon skeletons were identified from the aerial parts of *E. milii*. To the best of our knowledge, euphomilone A (**1**) is the first diterpenoid with 7/5/6 tricyclic system discovered in nature. Compound **2** is the first rosane-type diterpenoid with a 5/7/6 tricyclic system. The cyclic ether formed between C-10

DOI: 10.1021/acs.orglett.6b03142
Org. Lett. 2016, 18, 6132−6135

and C-19 in compound **3** is also the first found in the rosane-type diterpenoids. Altogether, these three new rosane-type diterpenoids increase the structural diversity of diterpenoids reported in the genus *Euphorbia* and provide new skeleton types for the future exploration of potential inhibitors of osteoclast formation.

■ ASSOCIATED CONTENT

Supporting Information

The Supporting Information is available free of charge on the ACS Publications website at DOI: 10.1021/acs.orglett.6b03142.

Experimental details, IR, ESIMS, HRESIMS, NMR, and computational data of **1**−**3** (PDF)
X-ray crystallographic data for compound **1** (CIF)
X-ray crystallographic data for compound **3**(CIF)

■ AUTHOR INFORMATION

Corresponding Author

*E-mail: guqiong@mail.sysu.edu.cn.

ORCID

Jun Xu: 0000-0002-1075-0337
Qiong Gu: 0000-0001-6011-3697

Author Contributions

⊥S.N.L. and D.H. contributed equally to this work.

Notes

The authors declare no competing financial interest.

■ ACKNOWLEDGMENTS

This study was supported in part by the National Natural Science Foundation of China (81573310), the Guangdong frontier and key technology innovation (Provincial Key Technology) project (2015B010109004), and the Medical Scientific Research Foundation of Guangdong Province (No. A2014212).

■ REFERENCES

(1) Vasas, A.; Hohmann, J. *Chem. Rev.* **2014**, *114*, 8579−8612.
(2) Shi, Q. W.; Su, X. H.; Kiyota, H. *Chem. Rev.* **2008**, *108*, 4295−4327.
(3) Wang, H. B.; Wang, X. Y.; Liu, L. P.; Qin, G. W.; Kang, T. G. *Chem. Rev.* **2015**, *115*, 2975−3011.
(4) Liang, Q. L.; Dai, C. C.; Jiang, J. H.; Tang, Y. P.; Duan, J. A. *Fitoterapia* **2009**, *80*, 514−516.
(5) Avila, L.; Perez, M.; Sanchez-Duffhues, G.; Hernandez-Galan, R.; Munoz, E.; Cabezas, F.; Quinones, W.; Torres, F.; Echeverri, F. *Phytochemistry* **2010**, *71*, 243−248.
(6) Keating, G. M. *Drugs* **2012**, *72*, 2397−2405.
(7) Zhang, X. Y.; Chen, E. H.; Li, R.; Yan, J. X.; Deng, Y. Q.; Tu, A. A.; Wang, P. Y.; Kong, J.; Ni, S. F. *J. Anhui Agri. Sci.* **2014**, *42*, 383−384.
(8) Cui, H.; Xu, B.; Wu, T. Z.; Xu, J.; Yuan, Y.; Gu, Q. *J. Nat. Prod.* **2014**, *77*, 100−110.
(9) Wu, T. Z.; Wang, Q.; Jiang, C.; Morris-Natschke, S. L.; Cui, H.; Wang, Y.; Yan, Y.; Xu, J.; Lee, K. H.; Gu, Q. *J. Nat. Prod.* **2015**, *78*, 500−509.
(10) Jiang, C.; Luo, P.; Zhao, Y.; Hong, J.; Morris-Natschke, S. L.; Xu, J.; Chen, C. H.; Lee, K. H.; Gu, Q. *J. Nat. Prod.* **2016**, *79*, 578−583.
(11) Gu, Q.; Chen, Y.; Cui, H.; Huang, D.; Zhou, J.; Wu, T. Z.; Chen, Y.; Shi, L.; Xu, J. *RSC Adv.* **2013**, *3*, 10168.
(12) Liu, X. T.; Pan, Q.; Shi, Y.; Williams, I. D.; Sung, H. H. Y.; Zhang, Q.; Liang, J. Y.; Ip, N. Y.; Min, Z. D. *J. Nat. Prod.* **2006**, *69*, 255−260.

DOI: 10.1021/acs.orglett.6b03142
Org. Lett. 2016, 18, 6132−6135